IJMTST | Volume: 2 | Issue: 07 | July 2016 | ISSN: 2455-3778

Hybrid Power Quality Compensator for Traction Power System with Photovoltaic Array

M. Kalidas[1] | B. Lavanya[2]

[1]PG Scholar, Department of Electrical & Electronics Engineering, Helapuri Institute of Technology and Science, Eluru, West Godavari (Dt), A.P, India.
[2]Assistant Professor, Department of Electrical & Electronics Engineering, Helapuri Institute of Technology and Science , Eluru, West Godavari (Dt), A.P, India.

ABSTRACT

A hybrid power quality compensator (HPQC) is proposed for comprehensive compensation under minimum dc operation voltage in high-speed traction power supplies. Reduction in HPQC operation voltage can lead to a decrease in the compensation device capacity, power consumptions, and installation cost. The parameter design procedures for minimum dc voltage operation of HPQC are being explored. It is shown through simulation results that similar compensation performances can be provided by the proposed HPQC with reduced dc-link voltage level compared to the conventional railway power compensator. The system rating thus can be reduced. The co phase traction power supply with proposed HPQC is suitable for high-speed traction applications. In this study, the renewable energy sources are used as the supply to the proposed concept. Since the solar radiation is abundant thought the world, we can use these systems any way. Renewable energy resources (RES) are being increasingly connected in distribution systems utilizing power electronic converters. The compensation performance of the proposed active power filter and the associated PV system generation scheme with new control scheme is demonstrated to improve the power quality features is simulated using MATLAB/ SIMULINK.

KEYWORDS: *PV, Co phase system, power quality compensator, reactive power compensation, traction power, unbalance compensation.*

I. INTRODUCTION

In traction power supply system's various techniques have been proposed to solve the system unbalance problem and also to increase the reliability of the system. When balanced transformers such as Scott and roof-delta transformers are used the system unbalance problem can be relieved. But with dynamic traction loads, the system balance cannot be maintained and compensation is required by the system to improve the power quality and also to reduce the total harmonic distortion (THD) of the system than which is present conventionally. This in turn improves the system operation [1-3].

The construction of special transformers to maintain system balance can add to the total installation cost of the system and we may not be able to solve the problem of reactive power and harmonics. Active compensators when compared to passive can provide better dynamic balance and comprehensive compensation under unbalance conditions [4].

Generally a Railway power compensator (RPC) is used in railway systems which can provide fast reactive power and harmonics compensation in traction power supply systems which solves the problem of excessive neutral sections installation in traction power supply systems. But its Total harmonic distortion value is high and provides poor power quality. Thus there is need for a device which is capable of providing better compensation and improved performance.

By the elimination of neutral sections the velocity loss of the locomotives can be reduced [4-6]. To avoid risk of phase mixing loads are connected across the same single phase output in these systems. Passive power quality compensators such

as reactive power compensation capacitors and passive filters are used in some systems to overcome the disadvantage of using active compensation. But the disadvantage of a passive equipment is that it cannot adjust the capability flexibly, where compensation problems occur frequently due to the frequent change in load [7]. The cost is low of the former, but the poor dynamic performance; the latter is real-time, but the cost is high. Combine the features of both, the literature, passive and active hybrid integrated compensation was proposed. At the same time, compensation characteristics and capacity configuration are discussed, but they did not cancel the secondary side of the transformer commutation link. In this paper, a hybrid device combining active and passive compensators, named as the hybrid power quality compensator (HPQC), is proposed for compensation in co phase traction power supply. The parameter design procedure for minimum HPQC voltage operation as well as the minimum voltage rating achievable is discussed [8-10].

II. Conventional and Proposed System Circuit Configurations

In this paper, the substation transformer is composed of two single-phase transformers, and is commonly known as the V/V transformer. The three-phase power grid is transformed into two single-phase outputs (Vac and Vbc phases) through V/V transformer. The locomotive loadings are all connected across the same single phase output (Vac), leaving another phase (Vbc) unloaded. The RPC is composed of one back-to-back converter and is connected across the Vac and Vbc phases, so as to provide power quality compensation for the system. The circuit configuration of the proposed co phase traction power supply with HPQC is shown in Fig. 1. In contrast to conventional structure, the converter is connected to the Vac phase of the transformer via a capacitive coupled hybrid LC structure. As will be discussed later, this results in the reduction of converter dc bus voltage of HPQC. The compensation algorithm of the proposed HPQC is similar to that in conventional RPC and is not discussed here. Details may be found. For better understanding of the discussions, the detailed structure and physical definitions of RPC in the conventional structure and HPQC in the proposed structure are presented in Fig. 2.

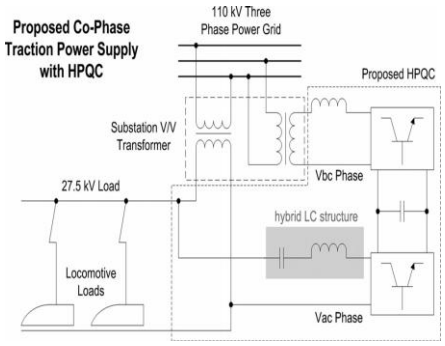

Fig.1. Circuit configuration of the proposed co phase traction power supply with HPQC.

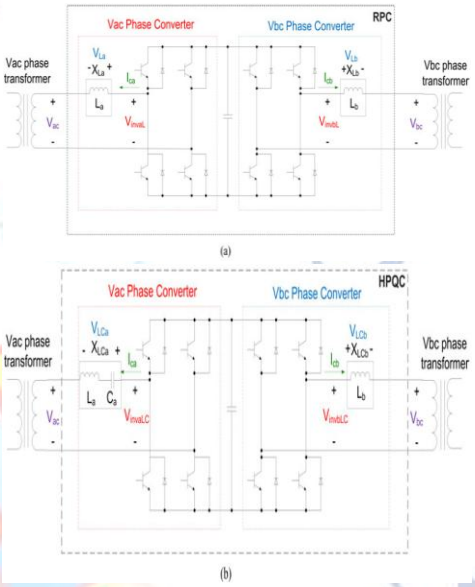

Fig.2. Detailed structure and physical definitions of (a) RPC in the conventional co phase traction power and (b) HPQC in the proposed co phase traction power.

Since traction loads are mostly inductive, the following contents are discussed based on the assumption of inductive loadings. The vector diagrams of the Vac phase converter for the conventional RPC and proposed HPQC are shown in Fig. 3. It can be observed that with capacitive coupled LC structure, the amplitude of Vinva LC in HPQC can be less than that of Vinva L in RPC under the same compensation current. The corresponding mathematical expressions are shown in (1) and (2). With capacitive coupled structure in HPQC, XLCa is of negative value, and it results in reduction of Vinva LC. Details of compensation current in co phase traction power may be found.

$$|V_{\text{inva}L}| = \sqrt{V_{\text{inva}Lp}^2 + V_{\text{inva}Lq}^2} = \sqrt{(V_{ac} + |I_{caq}|X_{La})^2 + (|I_{cap}|X_{La})^2} \quad (1)$$

$$|V_{\text{inva}LC}| = \sqrt{V_{\text{inva}LCp}^2 + V_{\text{inva}LCq}^2} = \sqrt{(V_{ac} + |I_{caq}|X_{LCa})^2 + (|I_{cap}|X_{LCa})^2} \quad (2)$$

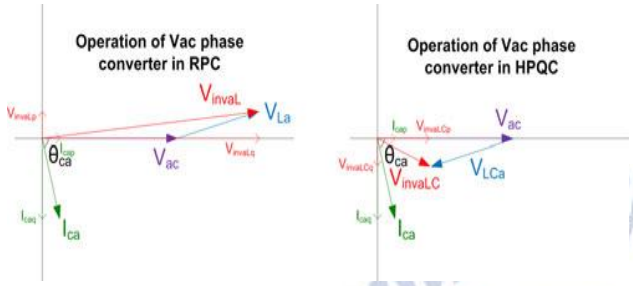

Fig.3 Vector diagram showing the operation of Vac phase converter in (a) RPC of the conventional structure and (b) HPQC of the proposed structure.

Vac coupled impedance in RPC and HPQC under load PF of 0.85 .The figure shows clearly that under the examined condition, the value of Vinva L in RPC is higher than that of Vinva LC in HPQC. Moreover, there is a minimum voltage operation point for HPQC. For instance, with load PF of 0.85, the minimum value of Vinva LC in HPQC is approximately 48% of Vac phase voltage. The operation point can be tuned along the curve by changing the Vac coupled impedance. Therefore, the HPQC operation could be located at the minimum voltage operation point via specific parameter design. The detailed discussions are given in the next section.

III. HPQC Parameter Design for the Minimum DC Voltage Operation

The parameter design for the minimum dc voltage operation of HPQC in the proposed structure is being explored in this section. The design procedures of Vac and Vbc phase coupled impedance are introduced, together with the investigations on the minimum HPQC dc voltage rating achievable.

A. Vac Phase Coupled Impedance Design

The vector diagram showing the operation of Vac phase converter in HPQC under minimum voltage operation. With constant load PF and capacity, the vector Ica is fixed. Thus, the vector VLca would vary along the line L1 as the Vac coupled impedance XLCa varies. It can be observed that the amplitude of Vinva LC can be minimized when it is perpendicular to the vector VLCa. In other words, the minimum amplitude of Vinva LC occurs when the compensation current Ica is in phase with the voltage Vinva LC. By further defining the power angle of Ica as θca, the mathematical relationship in (3)

$$V_{LCa}\,[V_{\text{inva}LC\_\min}] = I_{ca}X_{LCa} = V_{ac}\,(\sin\theta_{ca}) \quad (3)$$

The corresponding Vac coupled impedance XLCa required for minimum Vinva LC can, thus, be determined as shown in

$$X_{LCa}\,[V_{\text{inva}LC\_\min}] = \frac{V_{ac}\,(\sin\theta_{ca})}{I_{ca}} \quad (4)$$

With the aforementioned analysis, only the Vac coupled impedance design for minimum HPQC voltage operation is determined. However, the ultimate goal of a parameter design is to determine the Vac phase coupled inductance La and capacitance Ca for practical application. The linkage of XLCa with Ca and La can be obtained through circuit analysis, as shown in

$$X_{LCa}\,[V_{\text{inva}LC\_\min}] = \frac{V_{ac}\,(\sin\theta_{ca})}{I_{ca}} = -\left(\frac{\omega^2 L_a C_a - 1}{\omega C_a}\right) \quad (5)$$

For example, with Vac of 27.5 kV, load PF of 0.85, and capacity of 15 MVA, the variation of La and Ca which satisfies the relationship in (5) is presented. It can be observed that the relationship between La and Ca for minimum HPQC voltage rating is nonlinear. It is more practical for smaller physical size of lower inductance value. Furthermore, there is a limitation on the value of Ca, which is indicated by the large dot. This is also the Ca value boundary. For a Ca value exceeding this boundary, the HPQC drops into the inductive coupled region, causing the operation similar to RPC. Minimum voltage operation in HPQC, thus, fails when the value of Ca is outside this boundary.

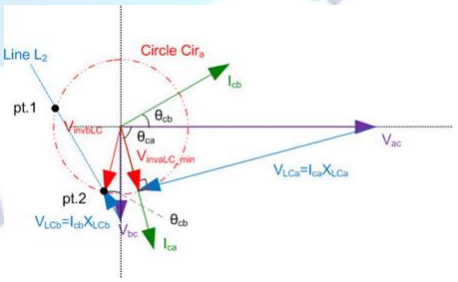

Fig. 4.Vector diagram showing the operation of HPQC in correspondence with minimized Vinva LC.

B. Vbc Phase Coupled Impedance Design

For the Vbc phase coupled impedance design, it is determined with matching to the minimum voltage Vinva LC min. The vector diagram showing the operation of Vbc phase converter in HPQC in correspondence with the Vinva LC min is shown in Fig. 4. The minimum HPQC voltage is represented

by the circle Cira with radius Vinva LC min. assuming constant load PF and capacity, the vector VLC b varies along the line L2 with varying Vbc phase coupled impedance XLCb. Two intersection points (pt.1 and pt.2) are present between the circle Cira and the line L2. These two points are the operation points which satisfy the voltage matching with Vinva LC min. They may be determined mathematically. The mathematical expression showing the intersection of circle Cira and the line L2 is given in

$$V_{\text{invaLC\_min}}^2 = (V_{LCb}^2 \sin^2\theta_{cb} + (V_{bc} - V_{LCb}\cos\theta_{cb})^2) \quad (6)$$

By solving the expression, the mathematical expressions for pt.1 and pt.2 can be obtained in

$$\text{(pt.2)}\ \frac{V_{bc}\cos\theta_{cb} - \sqrt{V_{\text{invaLC\_min}}^2 - V_{bc}^2\sin^2\theta_{cb}}}{I_{cb}} = X_{LCb}$$
$$= \frac{V_{bc}\cos\theta_{cb} + \sqrt{V_{\text{invaLC\_min}}^2 - V_{bc}^2\sin^2\theta_{cb}}}{I_{cb}}\ \text{(pt.1)} \quad (7)$$

Although both pt.1 and pt.2 may satisfy the voltage matching with Vinva LC min, operation point at pt.2 is preferred due to the lower impedance of XLCb and lower power consumptions. Besides the Vbc coupled impedance of XLCb, there is another issue concerning about the value of Vbc. For the circle Cira to have intersections with the line L2, the expression for XLCb in (7) must be real values. Thus, the restrictions in (8) can thus be obtained

$$V_{bc} \le \frac{V_{\text{invaLC\_min}}}{\sin\theta_{cb}} \quad (8)$$

C. Minimum HPQC Voltage Rating Achievable

After investigations of the *Vac* and *Vbc* phase coupled impedance design for the minimum HPQC operation voltage, the minimum voltage rating achievable is discussed in this section.

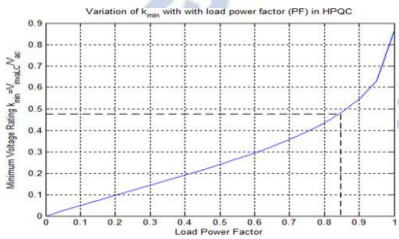

Fig. 5.Curve showing the variation of HPQC minimum voltage rating (k_min) with load PF.

The value of V_{inva} LC min is a key factor in the minimum HPQC voltage rating achievable. By substituting the design of Vac coupled impedance XLC an in (4) into the HPQC Vinva LC voltage calculation in (2), the minimum value of V_{inva} LC in HPQC (V_{inva} LC min) can be obtained in

$$V_{\text{invaLC\_min}} = (\cos\theta_{ca})V_{ac} \quad (9)$$

Neglecting the effect of Vac phase voltage, the minimum HPQC voltage rating is determined by

$$k_{\min} = \frac{V_{\text{invaLC\_min}}}{V_{ac}} = \cos\theta_{ca} \quad (10)$$

It is now obvious that the minimum HPQC voltage rating is dependent only on the power angle of Ica. This again correlates with the load PF, as expressed in

$$\theta_{ca} = \tan^{-1}\left(\frac{\frac{1}{2\sqrt{3}}\text{PF} + \sin(\cos^{-1}(\text{PF}))}{\frac{1}{2}\text{PF}}\right) \quad (11)$$

The curve showing the variation of minimum HPQC voltage rating (k_{min}) against load PF is plotted. It is equivalent to joining all the minimum operation points of the mesh plot. Under different load PF. For example, with load PF of 0.85, the minimum voltage rating is approximately 0.48, which is consistent with the analysis in Section II. Assuming Vac phase voltage of 27.5 kV, the minimum value of V_{inva} LC achievable is, thus, 13.2 kV. The peak Value of the Vac phase voltage is 38.89 kV, and the minimum HPQC dc-link voltage required is √2 times of V_{inva} LC, which is approximately 18.67 kV.

IV. Control Philosophy

The control block of the system is shown in Fig. 6. The instantaneous load active and reactive power is computed using the modified instantaneous pq theory.

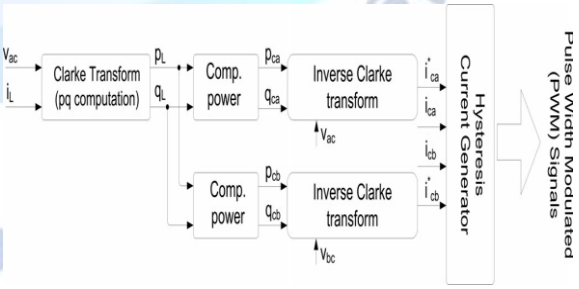

Fig. 6.Control block diagram of the HPQC for co phase traction power supply compensation.

The mathematical expression is shown in (12), in which V_{ac} and i_L are the load voltage and current rms, while V_{acd} and i_{Ld} are 90◦ delay of load voltage and current, respectively. p_L and q_L refer to the instantaneous load active (real) and reactive (imaginary) power.

$$\begin{bmatrix} p_L \\ q_L \end{bmatrix} = \begin{bmatrix} v_{ac} \cdot i_L + v_{acd} \cdot i_{Ld} \\ v_{acd} \cdot i_L - v_{ac} \cdot i_{Ld} \end{bmatrix}$$

The active power part p_L can be split into dc part p_{dc} which corresponds to the fundamental average active load power; and oscillating part p_{ac} which corresponds to the oscillating active power between system source and load and contributes as part of harmonics and reactive power (which need to be compensated). The mathematical expression is shown in

$$p_L = p_{dc} + p_{ac}$$

The required compensation power is then computed according to the power quality requirement, as expressed in (14), where p_{ca} and q_{ca} are the required active and reactive compensation power from the Vac phase converter, while p_{cb} and q_{cb} are the required active and reactive compensation power from the Vbc phase converter

$$\begin{bmatrix} p_{ca} \\ q_{ca} \\ p_{cb} \\ q_{cb} \end{bmatrix} = \begin{bmatrix} \frac{1}{2}p_{dc} + p_{ac} \\ \frac{1}{2\sqrt{3}}p_{dc} + q \\ -\frac{1}{2}p_{dc} \\ -\frac{1}{2\sqrt{3}}p_{dc} \end{bmatrix}.$$

The reference of V_{ac} and V_{bc} phase compensation current, i^*_{ca} and i^*_{cb}, can then be computed according to (15) and (16), where V_{bc} and V_{bcd} are the V_{bc} phase voltage and its 90◦ delay value

$$i^*_{ca} = \frac{1}{v_{ac}^2 + v_{acd}^2} \begin{bmatrix} v_{ac} & v_{acd} \end{bmatrix} \begin{bmatrix} p_{ca} \\ q_{ca} \end{bmatrix}$$

$$i^*_{cb} = \frac{1}{v_{bc}^2 + v_{bcd}^2} \begin{bmatrix} v_{bc} & v_{bcd} \end{bmatrix} \begin{bmatrix} p_{cb} \\ q_{cb} \end{bmatrix}$$

The computed reference current signal is then sent to the hysteresis current controller, which pulse width modulated signals are generated for the electronic switches of V_{ac} and V_{bc} phase converters. The HPQC balances the grid-side current by transferring active power from the V_{ac} phase to the V_{bc} phase. Meanwhile, harmonic and reactive power compensations are achieved by the V_{ac} phase converter.

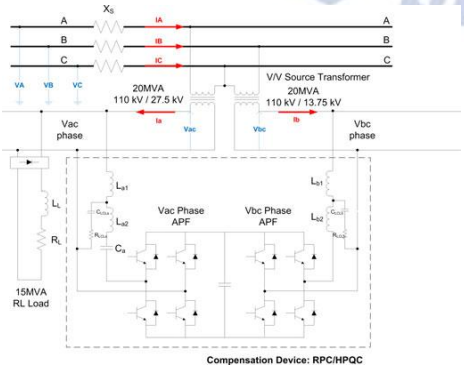

Fig.7.Circuit schematic of the system under investigated in simulation verifications.

Concerning the design of the LC filter parameter, it is selected so as to reduce the harmonics compensation capacity of the compensator. Although the highest load harmonic contents are located at the third harmonic frequency, the LC filter is tuned at the second highest load harmonics (fifth harmonic) for smaller physical size of the components.

V. PHOTOVOLTAIC SYSTEM

A Photovoltaic (PV) system directly converts solar energy into electrical energy. The basic device of a PV system is the PV cell. Cells may be grouped to form arrays. The voltage and current available at the terminals of a PV device may directly feed small loads such as lighting systems and DC motors or connect to a grid by using proper energy conversion devices.

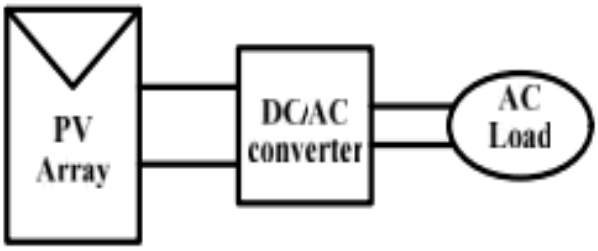

Fig.8. Block diagram representation of Photovoltaic system.

This photovoltaic system consists of three main parts which are PV module, balance of system and load. The major balance of system components in this systems are charger, battery and inverter. The Block diagram of the PV system is shown in Fig.8. A photovoltaic cell is basically a semiconductor diode whose p–n junction is exposed to light. Photovoltaic cells are made of several types of semiconductors using different manufacturing processes. The incidence of light on the cell generates charge carriers that originate an electric current if the cell is short circuited1

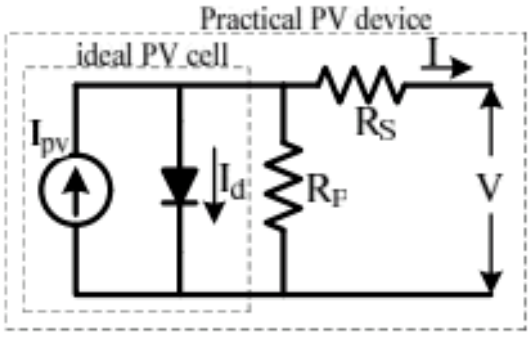

Fig.9. Practical PV device

The equivalent circuit of PV cell is shown in the fig.9. In the above figure the PV cell is represented

by a current source in parallel with diode. Rs and Rp represent series and parallel resistance respectively. The output current and voltage form PV cell are represented by I and V. The I-V characteristics of PV cell are shown in fig.10. The net cell current I is composed of the light generated current IPV and the diode current ID.

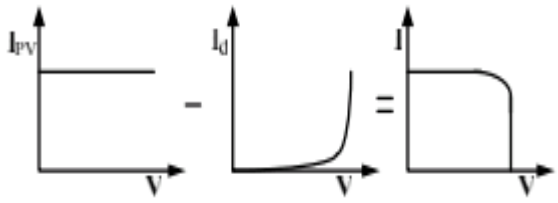

Fig.10. Characteristics I-V curve of the PV cell

VI. MATLAB/SIMULINK RESULTS

Here the simulation is carried out by different cases are shown in this chapter by using Matlab/simulink software

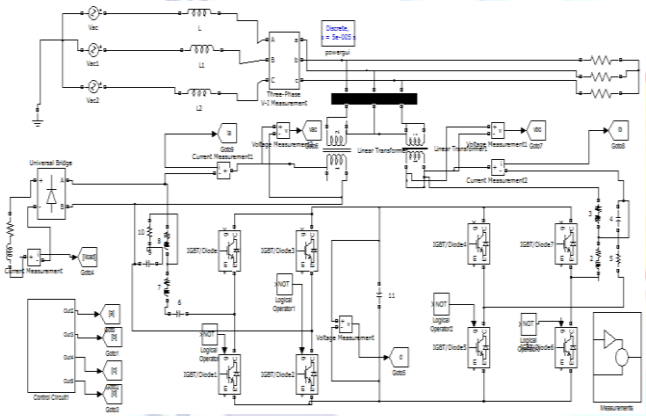

Fig.11. Matlab/simulink model of proposed co-phase traction power model

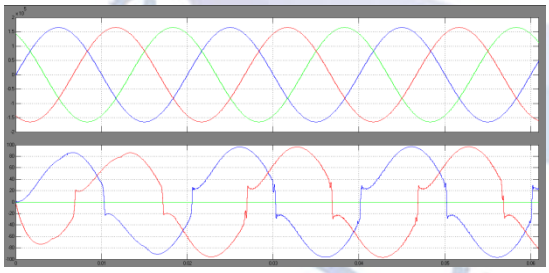

(a)

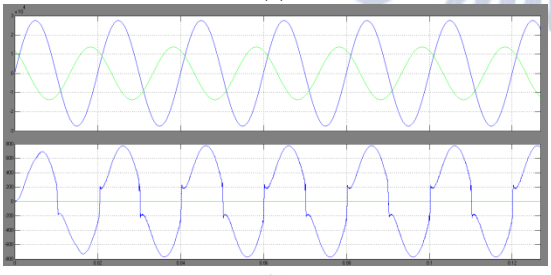

(b)

Fig.12. System performances of the proposed co-phase traction power without compensation (a) Three-phase power source voltage and current waveforms. (b) *Vac* and *Vbc* phase voltage and current waveforms

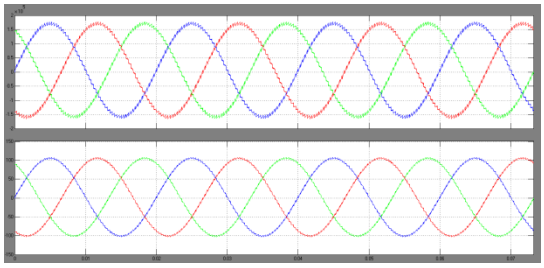

(a)

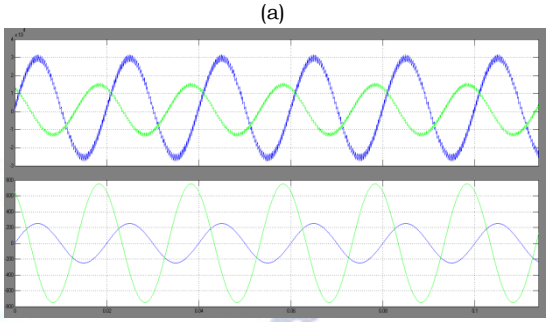

(b)

Fig. 13. System performances of cophase traction power with RPC (Vdc = 41 kV). (a) Three-phase power source voltage and current waveforms. (b) Vac and Vbc phase voltage and current waveforms.

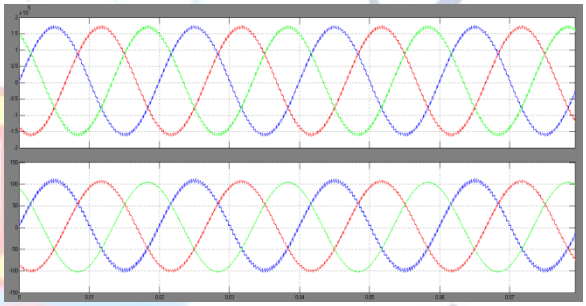

(a)

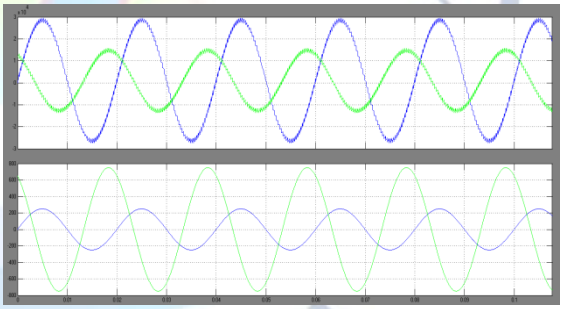

(b)

Fig. 14. System performances of the proposed co-phase traction power supply system with HPQC (Vdc = 27 kV). (a) Three-phase power source voltage and current waveforms. (b) Vac and Vbc phase voltage and current waveforms.

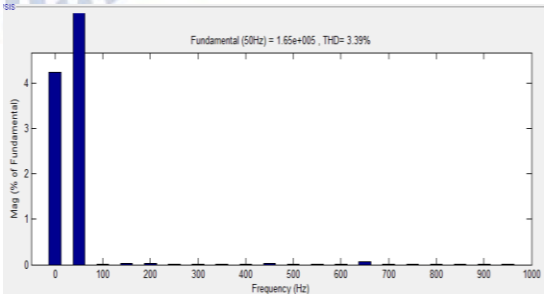

Fig.15. shows the total harmonic content by using PI is 3.39%

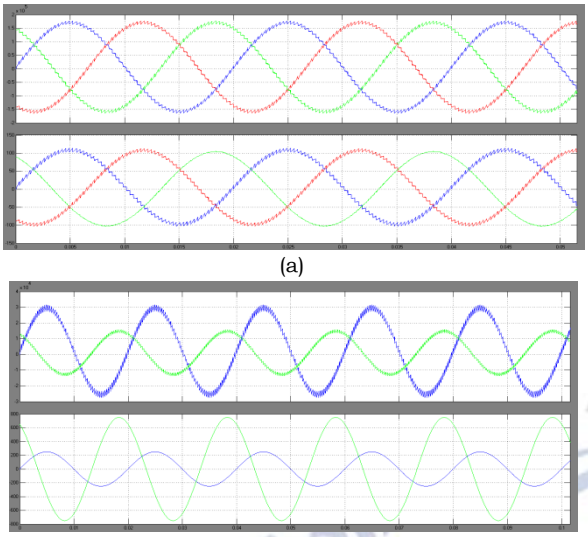

Fig.16. System performances of the proposed cophase traction power supply system with HPQC (V_{dc} = 41 kV). (a) Three-phase power source voltage and current waveforms. (b) V_{ac} and V_{bc} phase voltage and current waveforms.

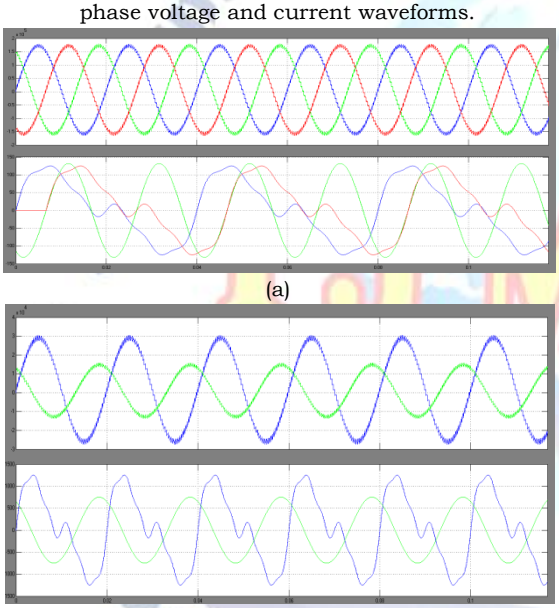

Fig. 17. System performances of the proposed cophase traction power supply system with HPQC (V_{dc} = 22 kV). (a) Three-phase power source voltage and current waveforms. (b) V_{ac} and V_{bc} phase voltage and current waveforms.

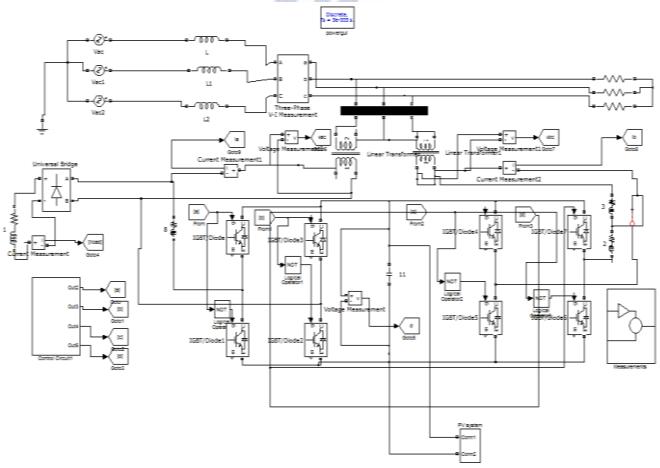

Fig.18. shows the Matlab/simulink model of Proposed Converter with Photovoltaic.

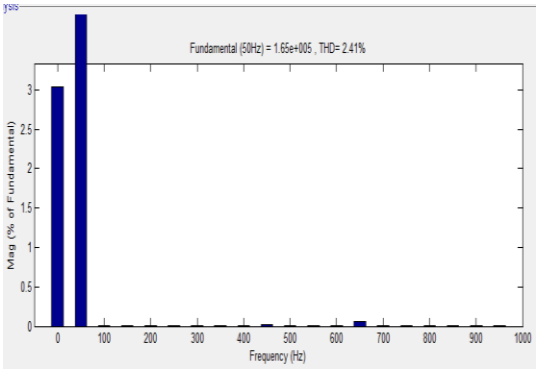

Fig.19. shows the total harmonic content.

VII. Conclusion

The PV system with shunt controller has been presented. The PV converter is voltage controlled with a repetitive algorithm. An MPPT algorithm has specifically been designed for the proposed voltage-controlled converter. It is based on the incremental conductance method, and it has been modified to change the phase displacement between the grid voltage and the converter voltage, thus maximizing the power extraction from the PV panels. The designed PV system provides grid voltage support at fundamental frequency and compensation of harmonic distortion at the point of common coupling. A HPQC with reduced dc voltage operation compared to conventional RPC during compensation is proposed in this paper. The parameter design for the minimum HPQC voltage operation is being discussed, and the minimum HPQC voltage operation point achievable is explored. Finally, all simulations results are verified through Matlab/Simulink software.

References

[1] P. E. Sutherland, M. Waclawiak, and M. F. McGranaghan, "System impacts evaluation of a single-phase traction load on a 115-kV transmission system," IEEE Trans. Power Delivery, vol. 21, no. 2, pp. 837–844, Apr. 2006

[2] H. Y. Kuo and T. H. Chen, "Rigorous evaluation of the voltage unbalance due to high-speed railway demands," IEEE Trans. Veh. Technol., vol. 47, no. 4, pp. 1385–1389, Nov. 1998.

[3] D. C. Howroyd, "Public-supply-system distortion and unbalance from single-phase a.c. traction," Proc. Inst. Electr. Eng., vol. 124, no. 10, pp. 853–859, 1977.

[4] IEEE Recommended Practice for Monitoring Electric Power Quality, IEEE Standard 1159-1995.

[5] IEEE Recommended Practices and Requirements for Harmonic Control in Electrical Power Systems IEEE Standard 519-1992.

[6] S. T. Senini and P. J.Wolfs, "Novel topology for correction of unbalanced load in single phase

electric traction systems," in Proc. IEEE 33rd Annu. Power Electron. Spec. Conf., Jun. 2002, vol. 3, pp. 1208–1212.

[7] Z. Zhang, B. Wu, J. Kang, and L. Luo, "A multi-purpose balanced transformer for railway traction applications," IEEE Trans. Power Delivery, vol. 24, no. 2, pp. 711–718, Apr. 2009.

[8] H. Wang, Y. Tian, and Q. Gui, "Evaluation of negative sequence current injection into the public grid from different traction substation in electrical railways," in Proc. 20th Int. Conf. Exhib. Electr. Distrib.—Part 1, 2009, pp. 1–4.

[9] C. Dai and Y. Sun, "Investigation of the imbalance current compensation for transformers used in electric railways," in Proc. Asia-Pacific Power Energy Eng. Conf., 2010, pp. 1–4.

[10] Z. Sun, X. Jiang, D. Zhu, and G. Zhang, "A novel active power quality compensator topology for electrified railway," IEEE Trans. Power Electron., vol. 19, no. 4, pp. 1036–1042, Jul. 2004.